Preface for Applied Scanning Probe Methods Vol. XI–XIII

The extremely positive response by the advanced community to the Springer series on Applied Scanning Probe Methods I–X as well as intense engagement of the researchers working in the field of applied scanning probe techniques have led to three more volumes of this series. Following the previous concept, the chapters were focused on development of novel scanning probe microscopy techniques in Vol. XI, characterization, i.e. the application of scanning probes on various surfaces in Vol. XII, and the application of SPM probe to biomimetics and industrial applications in Vol. XIII. The three volumes will complement the previous volumes I–X, and this demonstrates the rapid development of the field since Vol. I was published in 2004. The purpose of the series is to provide scientific background to newcomers in the field as well as provide the expert in the field sound information about recent development on a worldwide basis.

Vol. XI contains contributions about recent developments in scanning probe microscopy techniques. The topics contain new concepts of high frequency dynamic SPM technique, the use of force microscope cantilever systems as sensors, ultrasonic force microscopy, nanomechanical and nanoindentation methods as well as dissipation effects in dynamic AFM, and mechanisms of atomic friction.

Vol. XII contains contributions of SPM applications on a variety of systems including biological systems for the measurement of receptor–ligand interaction, the imaging of chemical groups on living cells, and the imaging of chemical groups on live cells. These biological applications are complemented by nearfield optical microscopy in life science and adhesional friction measurements of polymers at the nanoscale using AFM. The probing of mechanical properties by indentation using AFM, as well as investigating the mechanical properties of nanocontacts, the measurement of viscous damping in confined liquids, and microtension tests using in situ AFM represent important contributions to the probing of mechanical properties of surfaces and materials. The atomic scale STM can be applied on heterogeneous semiconductor surfaces.

Vol. XIII, dealing with biomimetics and industrial applications, deals with a variety of unconventional applications such as the investigations of the epicuticular grease in potato beetle wings, mechanical properties of mollusc shells, electrooxidative lithography for bottom-up nanofabrication, and the characterization of mechanical properties of biotool materials. The application of nanomechanics as tools for the investigation of blood clotting disease, the study of piezo-electric polymers, quantitative surface characterization, nanotribological characterization of

carbonaceous materials, and aging studies of lithium ion batteries are also presented in this volume.

We gratefully acknowledge the support of all authors representing leading scientists in academia and industry for the highly valuable contribution to Vols. XI–XIII. We also cordially thank the series editor Marion Hertel and her staff members Beate Siek and Joern Mohr from Springer for their continued support and the organizational work allowing us to get the contributions published in due time.

We sincerely hope that readers find these volumes to be scientifically stimulating and rewarding.

August 2008   Bharat Bhushan
                                                              Harald Fuchs

10 Imaging Chemical Groups and Molecular Recognition Sites on Live Cells Using AFM

David Alsteens · Vincent Dupres · Etienne Dague · Claire Verbelen · Guillaume André · Grégory Francius · Yves F. Dufrêne

Abstract. Imaging the nanoscale distribution of specific chemical and biological sites on live cells is an important challenge in current life science research. In addition to imaging the surface topography of live cells, atomic force microscopy (AFM) is increasingly used to probe their chemical groups and biological receptors. In chemical force microscopy, AFM tips are modified with specific functional groups, thereby allowing investigators to probe chemical sites and their interactions on a scale of only ∼25 functional groups. In molecular recognition imaging, tips are functionalized with specific biomolecules, or samples labeled with immunogold particles, enabling researchers to localize specific receptors. Clearly, these nanoscale investigations provide new avenues in cellular biology and microbiology for elucidating the structure–function relationships of cell surfaces. In this chapter, we discuss the principles of these AFM modalities and their applications in life science research.

Key words: Atomic force microscopy, Cells, Chemical force microscopy, Molecular recognition studies, Single molecules

10.1 Introduction

Specific molecular recognition interactions between receptors and cognate ligands are ubiquitous in life sciences and increasingly used in nanobiotechnology [1–3]. In addition, nonspecific intermolecular interactions, such as hydrophobic and electrostatic forces, also play essential roles in biology since they promote crucial events like protein folding and cell adhesion [4, 5]. Despite the importance of these noncovalent intermolecular forces, their quantification has long been challenging. Force measuring techniques like the surface forces apparatus (SFA) [6] and the optical and magnetic tweezers [7, 8] have been increasingly used in that respect; yet these approaches are limited by their poor lateral resolution which does not provide access to the spatial distribution of (bio)chemical interactions. In this context, atomic force microscopy (AFM) has recently opened remarkable opportunities. On the one hand, chemical force microscopy (CFM), involving modification of AFM tips with specific functional groups, has enabled researchers to map the spatial arrangement of chemical groups and their interactions on organic surfaces and on cell surfaces. This nanoscale, chemically sensitive imaging tool offers two major advantages over classical probing methods: (1) hydrophobic and charged groups, and their interactions,

are measured directly and quantitatively on live cells, and (2) nanoscale variations of hydrophobicity and charge can be resolved. On the other hand, single-molecule force spectroscopy with biologically modified tips provides a means to map individual receptors on cellular surfaces and to measure their molecular recognition forces. As a complement, topographic imaging combined with immunogold labeling has also proved useful for localizing molecular recognition sites. In this chapter, we describe the principle and methodology of chemical force microscopy and molecular recognition imaging, and highlight some of their applications.

10.2
Chemical Force Microscopy

10.2.1
Methods

The general idea of CFM is to use AFM tips with well-defined chemistry for measuring adhesion and friction, and/or for imaging surfaces (for recent reviews [6, 9]). AFM cantilevers and tips are usually made of silicon (Si) or silicon nitride (Si_3N_4) using microfabrication techniques. Because the surface chemistry of such commercial tips is poorly controlled and often contaminated with gold and other materials, reliable CFM measurements require functionalizing the tip surface with organic monolayers terminated by specific functional groups (e.g., OH or CH_3). A common method to achieve this is based on the formation of self-assembled monolayers (SAMs) of alkanethiols on gold surfaces. The procedure involves coating, by thermal evaporation, microfabricated cantilevers with a thin adhesive layer (Cr or Ti), followed by a 15–100-nm thick Au layer, immersing the coated cantilevers in dilute (0.1–1 mM) ethanol solutions of the selected alkanethiol, rinsing with ethanol and drying, using a gentle nitrogen flow. Although the protocol is fairly simple, it is important to validate the quality of the surface modification, which can be done by treating model supports (silicon) in the same way as the tips and characterizing them by means of surface analysis techniques (e.g., contact angle measurements or X-ray photoelectron spectroscopy). Another important point is to use the functionalized tips immediately after they are prepared in order to minimize surface contamination and alteration.

The most common application of CFM is the measurement of the adhesion strength between chemical groups via force spectroscopy. Here, the cantilever deflection is recorded as a function of the vertical displacement of the piezoelectric scanner, i.e. as the sample is pushed towards the tip and retracted. This yields a raw "voltage-displacement" curve which can be converted into a "force-distance" curve as follows. Using the slope of the curves in the region where tip and sample are in contact, the voltage can be converted into a cantilever deflection. In order to minimize the possible effects of repulsive surface forces and/or sample deformation, it is recommended to consider the slope of the retraction curve. The cantilever deflection is then converted into a force (F) using Hooke's law: $F = -k \times d$, where k is the cantilever spring constant. The curve can be corrected by plotting F as a function of $(z - d)$. The zero separation distance is then determined as the position of the vertical linear

parts of the curve in the contact region. Note that force mapping can be performed by recording spatially resolved force-distance curves in the (x, y) plane. In adhesion measurements, the hysteresis or "pull-off" force observed during retraction is used to estimate the adhesion (unbinding) force between tip and sample. To get an accurate knowledge of the measured forces, it is important to determine actual spring constants experimentally since they may substantially differ from values quoted by the manufacturer [10].

10.2.2
Probing Hydrophobic Forces

A variety of chemical groups (hydrophobic/hydrophilic; charged/uncharged) and their interactions in different solvents have been investigated using CFM [9, 11–16]. Recently, Alsteens et al. [17–19] validated the use of the technique for probing hydrophobic groups and for quantifying short-range hydrophobic forces. Although hydrophobic forces have been known for 70 years and are of prime importance in biology (protein folding and aggregation, membrane fusion and cell adhesion), their detailed mechanisms are not fully understood. Various effects have been proposed to explain these forces, such as entropic effects due to disruption of the arrangement of water near hydrophobic surfaces (solvent organization), separation-induced phase transition (cavitation), hydrodynamic fluctuating correlation, bridging of submicron bubbles, electrostatic effects, correlated charge fluctuations or correlated dipole interactions.

As a proof of concept, SAMs of CH3- and OH-terminated alkanethiols mixed in different proportions were probed using water contact angle measurements and CFM with hydrophobic, CH3-terminated tips (Fig. 10.1). Consistent with the expectation (work of adhesion, Young equation), the contact angle and adhesion force values measured on mixed SAMs increased gradually with the molar fraction of CH3-terminated alkanethiols (Fig. 10.1a, b), yielding a linear relationship between the adhesion force and the cosine of the contact angle (Fig. 10.1c). This excellent agreement demonstrates that the measured adhesion forces reflect surface hydrophobicity, thus hydrophobic forces.

Notably, as we shall see below, interpretation of the data in terms of interfacial thermodynamics reveals that the measured adhesion forces do not originate from true, direct tip–sample interactions, but may rather reflect entropy changes associated with the restructuration of water near hydrophobic surfaces. We start by considering the Johnson–Kendall–Roberts (JKR) model which links the adhesion force (F_{adh}) to the work of adhesion (W_{adh}) [12]:

$$F_{adh} = 1.5\pi R W_{adh} \tag{10.1}$$

where R is the radius of curvature of the AFM tip. The work of adhesion in water is given by [20]:

$$
\begin{aligned}
W_{adh} &= \gamma_{sample,water} + \gamma_{tip,water} - \gamma_{tip,sample} \\
&= W_{tip,sample} - W_{sample,water} - W_{tip,water} + 2\gamma_{water}
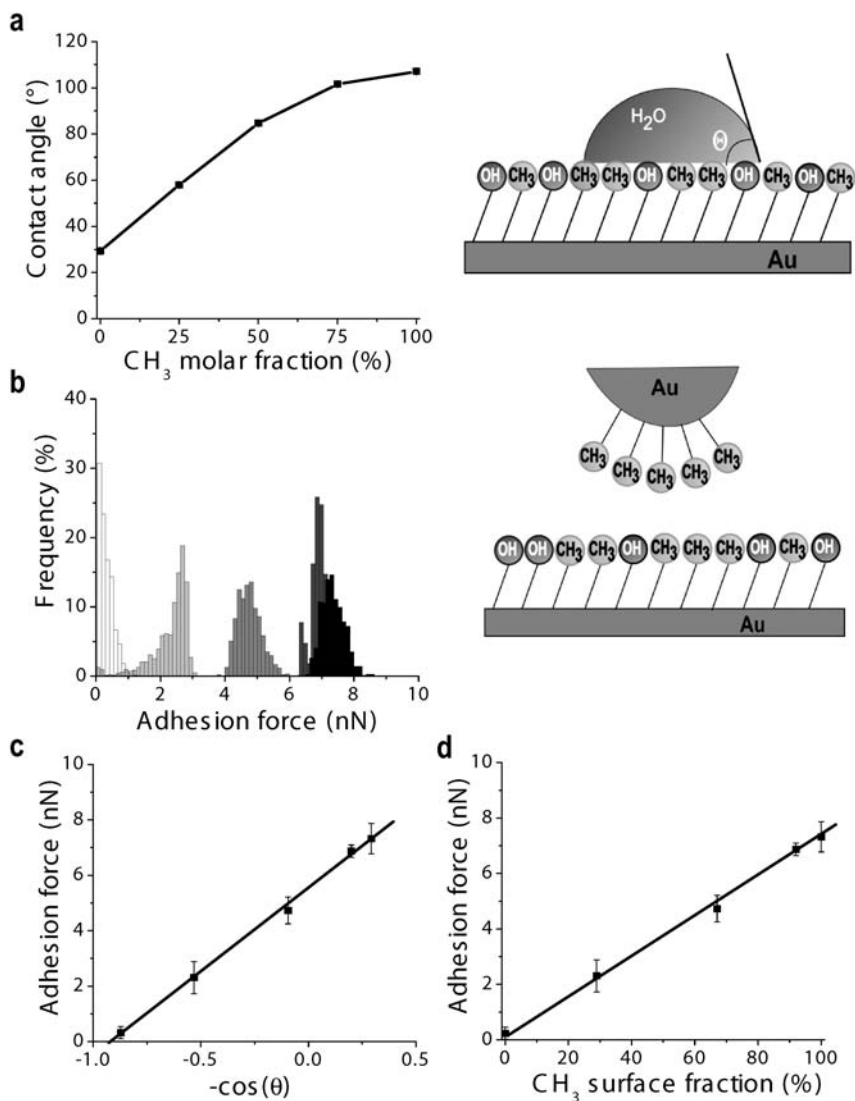\end{aligned}
\tag{10.2}
$$

Fig. 10.1. Chemical force microscopy (CFM): principle and application to the probing of hydrophobic forces. (**a**) Water contact angle (θ) values measured for mixed self-assembled monolayers of CH3- and OH-terminated alkanethiols as a function of the molar fraction of CH3-terminated alkanethiols. (**b**) Histograms of adhesion forces measured on the mixed SAMs using CFM with hydrophobic CH3-tips. (**c**) Variation of adhesion forces as a function of the cosine of the water contact angle. (**d**) Adhesion force as a function of the surface fraction of CH3-terminated alkanethiols computed using Cassie's law. Reprinted with permission from [17]

where $\gamma_{X,Y}$ is the interfacial energy, $W_{X,Y}$ is the work of adhesion in a vacuum, and γ_X is the surface energy. The term $W_{sample,water}$ can be deduced from the water contact angle θ, using the Young equation:

$$W_{sample,water} = \gamma_{sample} + \gamma_{water} - \gamma_{sample,water}$$
$$= \gamma_{water}(1 + \cos\theta) \tag{10.3}$$

Combining Eqs. (10.1), (10.2), and (10.3), yields the following expression:

$$\frac{F_{adh}}{1.5\pi R} = W_{tip,sample} - W_{tip,water} - \gamma_{water}\cos\theta + \gamma_{water} \tag{10.4}$$

Assuming that the $W_{tip,sample}$ and $W_{tip,water}$ values are close, which appears reasonable since the CH_3-modified tip is involved only in dispersion interactions (London forces) (10.4) becomes:

$$\frac{F_{adh}}{1.5\pi R} = \gamma_{water} - \gamma_{water}\cos\theta \tag{10.5}$$

Considering the surface tension of water (72.6 mN/m) and the tip radius ($\sim$20 nm) then leads to the following linear equation $F_{adh} = 6.84 - 6.84\cos\theta$, which agrees remarkably well with the regression equation of Fig. 10.1c, i.e.: $F_{adh} = 5.60 - 6.08\cos\theta$, where the uncertainties on slope and intercept are 0.14 and 0.10 nN, respectively. The agreement between experimental and theoretical adhesion forces supports the hypothesis that $W_{tip,sample}$ and $W_{tip,water}$ are similar, thus that only dispersion forces are responsible for the measured forces.

Accordingly, this reasoning indicates that the measured adhesion forces do not originate from true, direct tip–sample interactions, but may rather reflect entropy changes associated with the restructuration of water near hydrophobic surfaces. This work is also of practical interest since it shows that CFM can be used for quality control of chemically modified tips, which is not feasible by common analytical techniques. As we shall discuss below, further interpretation of cellular data implied expressing the measured adhesion force as a function of the surface fraction of CH_3-terminated alkanethiols, determined using Cassie's law and contact angle values (Fig. 10.1d).

In earlier work, AFM was also used to probe charged groups and their electrostatic forces [12, 13, 21]. For instance, force-distance curves were recorded at different pH values between tips and surfaces modified with carboxylic groups [22]. The curves showed differences according to pH (Fig. 10.2): while no adhesion was observed at pH 10, significant adhesion forces, of 1.4-nN magnitude, were measured at pH 3. Curves recorded in the 3–10 pH range showed adhesion forces for pH values smaller than 5. In addition, at pH 10 a long range repulsion force was seen starting at 40 nm, while a jump to contact was noted at pH 3. The repulsion force at high pH was attributed to electrostatic double layer forces between negatively charged COO^-/COO^- surfaces. The jump to contact at low pH was due to attractive van der Waals forces and indicated a lack of repulsion between uncharged COOH/COOH surfaces. In the same way, the strong adhesion observed at low pH values could be attributed to hydrogen bonding between COOH/COOH groups while the lack of adhesion at high pH was suggested to reflect the electrostatic repulsion
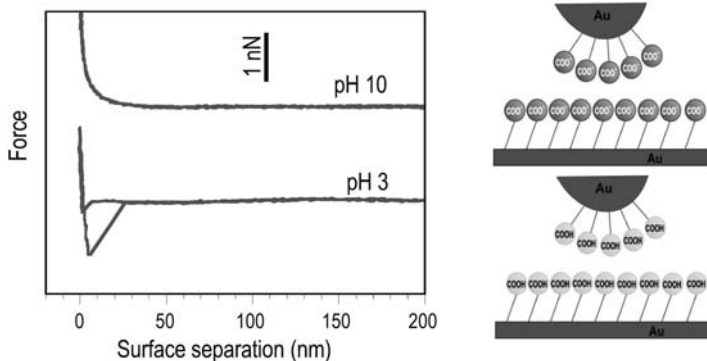
Fig. 10.2. AFM force-distance curves recorded at pH 10 and pH 3 between modified tips and model surfaces terminated with COOH groups. As shown in the drawing the differences observed according to pH can be related to a change of ionization state of the surfaces. Adapted with permission from [22]

between the negatively charged COO^-/COO^- surfaces. Hence, the above studies show that functionalized tips are very sensitive to hydrophobic and charged groups.

10.2.3
Chemical Force Microscopy of Live Cells

For the first time, we showed that the CFM technique can probe chemical groups and their interactions on live cells on a scale of only ∼25 functional groups [17–19, 23]. Dague et al. [19] used CFM with methyl-terminated tips to measure the hydrophobicity of the human opportunistic pathogen *Aspergillus fumigatus*. Topographic images revealed the presence of regularly arranged rodlets on *A. fumigatus* conidia (Fig. 10.3a). These structures are composed of hydrophobins, a family of small, moderately hydrophobic proteins that favor spore dispersion by air currents and mediate adherence to host cells. Force curves recorded across these surfaces with a hydrophobic tip showed large adhesion forces, of ∼3, 000 pN magnitude (Fig. 10.3b, c). Comparison with the data obtained on reference surfaces (Fig. 10.1d) indicated that the conidial surface has a marked hydrophobic character, corresponding to a surface composed of ∼10 CH_3 and ∼15 OH groups, which is fully consistent with the presence of an outermost surface layer of hydrophobins and provides direct indications as to their putative functions as dispersion and adherence structures. In agreement with the uniform surface structure, adhesion maps were rather homogeneous (Fig. 10.3b), supporting the idea that the *A. fumigatus* conidial surface is homogeneously hydrophobic.

Two hydrophilic controls confirmed that the measured hydrophobic properties are associated with hydrophobins [19]. First, topographic images recorded on conidia treated with NaOH, a procedure that removes all cell wall proteins including rodlet proteins, revealed a surface lacking any rodlet, but exposing underlying cell wall polysaccharides (Fig. 10.3d, e, f). These structural changes were correlated with profound decrease of cell surface hydrophobicity, the adhesion force towards the hydrophobic tip being only ∼300 pN. Second, similar results were obtained on the
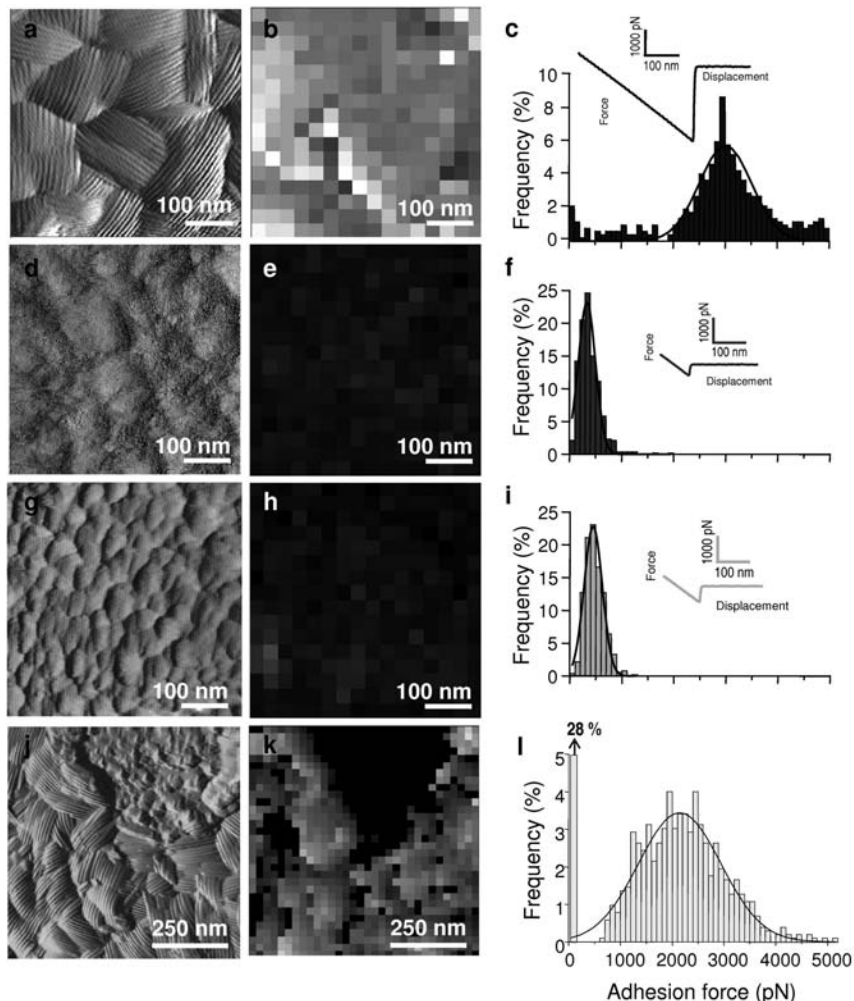
Fig. 10.3. CFM of *Aspergillus fumigatus*. (**a**) High-resolution image of a wild-type conidial surface in aqueous solution revealing rodlets. (**b**) Adhesion force map (*z*-range: 6 nN) and (**c**) adhesion force histogram (n = 512) recorded with a hydrophobic tip, indicating that the rodlet surface is uniformly hydrophobic. (**d**, **e**, **f**, **g**, **h**, **i**) High-resolution images, adhesion force maps and histograms (n = 512) obtained on NaOH-treated conidia (**d**, **e**, **f**) and on the ΔrodA ΔrodB double mutant (**g**, **h**, **i**). The purely hydrophilic surface is attributed to cell wall polysaccharides. (**j**, **k**, **l**) High-resolution image, adhesion force map and histogram obtained on SDS-treated conidia, revealing highly correlated structural and hydrophobic heterogeneities. Reprinted with permission from [19]

ΔrodA ΔrodB double mutant which does not produce rodlets (Fig. 10.3g, h, i). Considering the above reference SAMs surfaces (Fig. 10.1d), it was concluded that the two conidial surfaces are purely hydrophilic, corresponding to purely OH-terminated surfaces, which agrees well with the exposure of cell wall carbohydrates. Notably, nanoscale variations of hydrophobic properties were also resolved on SDS-treated

conidia, for which rodlet patches are missing in very localized regions (Fig. 10.3j, k, l). These nanoscale structural heterogeneities were directly correlated with differences in hydrophobicity, the rodlet and polysaccharide regions displaying contrasted hydrophobic and hydrophilic characters.

Remarkably, real-time CFM with a temperature-controlled stage enables researchers to probe not only structural, but also chemical dynamics on cells. In one such study, the changes of *A. fumigatus* conidia occurring during germination at 37 °C were tracked in real time (Fig. 10.4, [23]). Images of the same spore after 20 min, 60 min, and 120 min clearly revealed significant structural alterations, the rodlet layer changing into a layer of amorphous material, presumably reflecting the underlying polysaccharides. Consistent with this, adhesion maps with hydrophobic tips revealed a dramatic loss of hydrophobicity with time. After 2-h of germination, heterogeneous hydrophobic contrast was observed, reflecting the coexistence of hydrophobic rodlets and hydrophilic polysaccharides. These data nicely demonstrate that CFM is capable of resolving submicron chemical heterogeneities on live cells as they grow.

Of particular interest in the medical context, is the possibility to probe differences of chemical properties and interactions on cells following treatments with drugs. For instance, Alsteens et al. [18] showed that the surface of mycobacteria has a remarkably strong hydrophobic character due to the presence of an outermost layer of hydrophobic mycolic acids. This finding is of biomedical relevance since these hydrophobic constituents are thought to represent an important permeation barrier to common antibacterial agents. By contrast, treatment of the cells with two antibiotics, isoniazid and ethambutol, led to a dramatic decrease of cell surface hydrophobicity, attributed to the removal of the mycolic acid layer [18, 19]. Hence, the combination of topographic imaging with CFM provides unique opportunities to gain insight into the action modes of antibiotics as well as into the nanoscale organization of bacterial cell walls.

CFM has also been used to probe charged groups and their interactions on live cells, which is particularly relevant since most microorganisms possess a negative surface charge under physiological conditions due to the presence of anionic surface groups such as carboxyl and phosphate. The resulting cell surface charge plays an important role in controlling cell adhesion and aggregation phenomena, as well as antigen–antibody, cell–virus, cell–drug and cell–ions interactions. An example of this is provided by the work of Ahimou et al. [22] who used AFM tips functionalized with ionizable carboxyl groups to probe the electrostatic properties of *S. cerevisiae*. In Fig. 10.5, one can see that force-distance curves recorded in these conditions were strongly influenced by pH: while no adhesion was measured at neutral/alcaline pH,

--→

Fig. 10.4. Tracking the structural and chemical dynamics of germinating *A. fumigatus* cells. Series of high-resolution deflection images (*left*) and adhesion force maps (*right*) recorded on a single spore during germination. Within less than 3 h, the crystalline rodlet layer changed into a layer of amorphous material, presumably reflecting inner cell wall polysaccharides. After 2 h, both rodlet and amorphous regions were found to coexist (separated by *dashed line*). Consistent with this structural dynamics, substantial reduction of adhesion contrast was noted with time (*right* images), reflecting a dramatic decrease of hydrophobicity. After 2 h, heterogeneous contrast was observed in the form of hydrophobic patches (*dashed line*), surrounded by a hydrophilic sea. Reprinted with permission from [23]
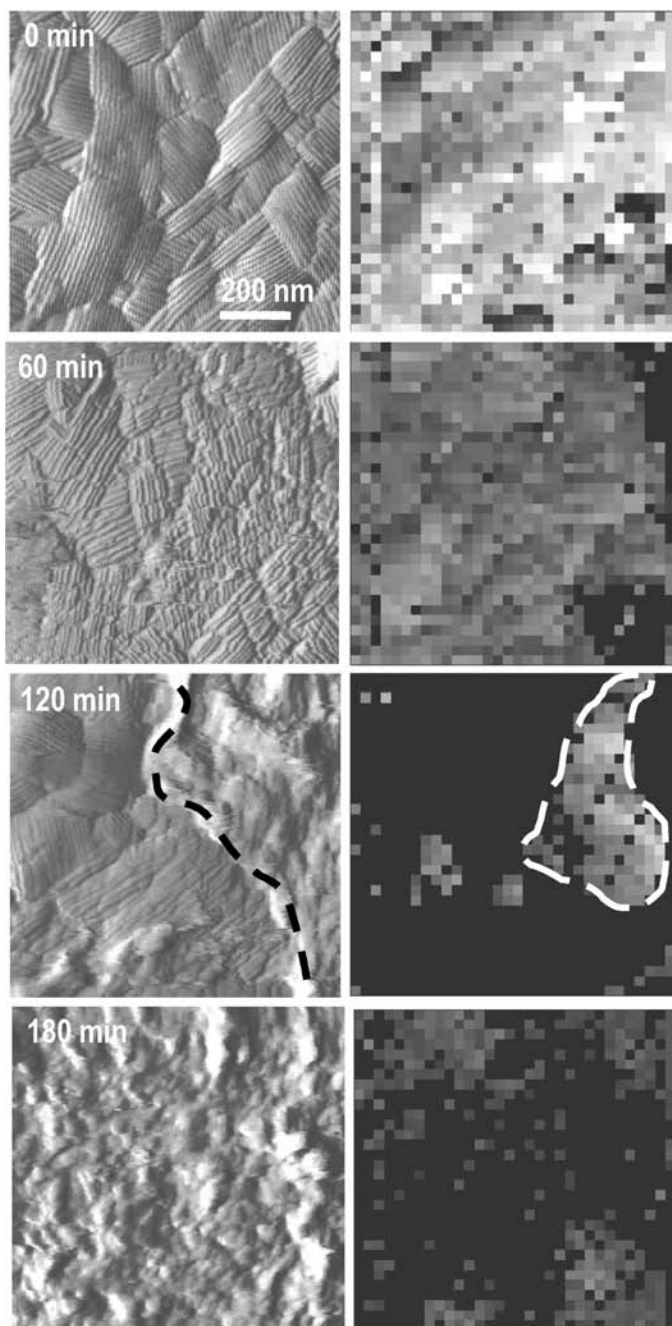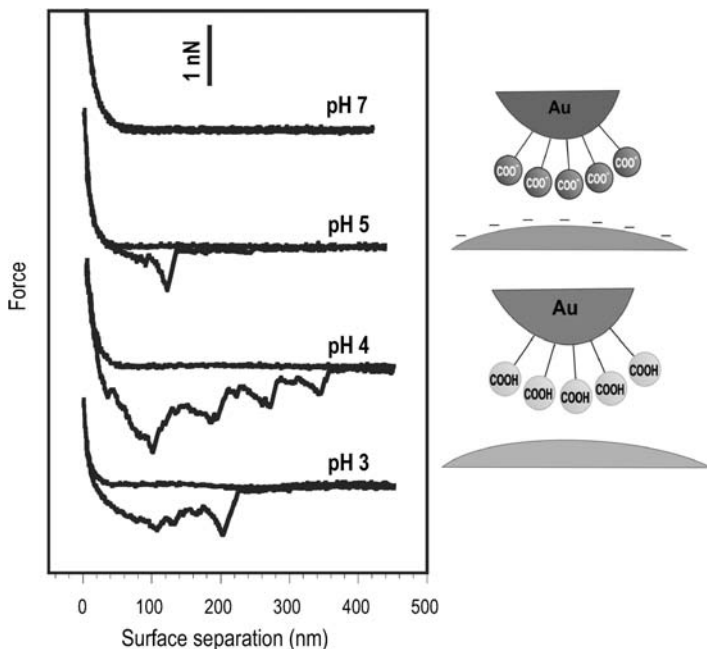
Fig. 10.4.

Fig. 10.5. Force-distance curves recorded in solutions of varying pH between the surface of *Saccharomyces cerevisiae* and an AFM tip functionalized with carboxyl groups. The differences in adhesion forces observed with pH were related to a change of ionization state of the cell surface. Adapted with permission from [22]

reflecting electrostatic repulsion between the negatively charged surfaces, multiple adhesion forces were recorded at pH ≤ 5 which we attribute to hydrogen bonding between the protonated tip surface and cell surface macromolecules. These changes were shown to be related to differences in the ionization state of the cell surface functional groups: the adhesion force *vs.* pH curve was correlated with microelectrophoresis data, the pH of the largest adhesion force corresponding to the cell isoelectric point (pH 4).

To summarize, the above data demonstrate that the CFM method allows investigators to detect specific chemical groups and measure their interaction forces on live cells, thereby complementing methods currently available for assessing surface properties. Also, the technique can resolve nanoscale chemical heterogeneities while the cells grow or interact with drugs.

10.3
Molecular Recognition Imaging

Single-molecule force spectroscopy (SMFS) with biologically modified tips enables us to measure molecular recognition interactions at the level of single molecules, providing valuable information on the molecular dynamics within the complexes, and

to map individual receptors on surfaces. In parallel, molecular recognition sites may also be detected using topographic imaging combined with immunogold labeling.

10.3.1
Spatially Resolved Force Spectroscopy

So-called "affinity imaging" using spatially resolved SMFS provides unique possibilities for the localization of specific receptors on cell surfaces. The method implies recording multiple force curves between the modified tip and sample, assessing the unbinding force between complementary receptor and ligand molecules from the adhesion "pull-off" force observed upon retraction, and displaying the values as gray pixels [24]. The measured unbinding forces are typically in the 50–400-pN range, depending on the experimental conditions, i.e. number of interacting molecules and the loading rate. The method has been applied to different cell types, including red blood cells [25], osteoclasts [26], and endothelial cells [27].

The power of the approach in microbiology is illustrated in Fig. 10.6 with three key examples. Flocculation (i.e. aggregation) of yeast cells in fermentation technology, such as brewing and wine-making, is mediated by specific lectin–carbohydrate interactions. To measure these interactions on *S. carlsbergensis*, AFM tips were functionalized with the plant lectin concanavalin A (Con A). As can be seen in Fig. 10.6b, the force curves obtained on top of a single yeast cell showed single or multiple unbinding forces of respectively $53 \pm 6\,pN$, $94 \pm 12\,pN$ and $145 \pm 17\,pN$ magnitude reflecting the specific interaction between one, two, and three lectins and cell surface mannose or glucose residues. In addition, the homogeneous adhesion maps suggested that the distribution of carbohydrate residues was homogeneous.

In the medical context, molecular recognition events mediate the interaction between adhesins on bacterial pathogens and host receptors. A prominent example is *M. tuberculosis* which adheres to heparan sulfates on epithelial cells via the heparin-binding hemagglutinin (HBHA). Spatially resolved SMFS was used to map the distribution of single HBHA on live mycobacteria (Fig. 10.6c, d; [28]). While high-resolution topographic images of the cells revealed a smooth and homogeneous surface, affinity maps recorded with a heparin-modified tip were highly contrasted (Fig. 10.6d), adhesion events (bright pixels) being observed in about half

Fig. 10.6. Molecular recognition imaging of live cells using spatially resolved SMFS. (**a**) AFM image of a *Saccharomyces carlsbergensis* cell showing a homogeneous, smooth morphology. (**b**) Adhesion force map (*gray scale*: 200 pN) recorded with an AFM tip functionalized with the plant lectin concanavalin A, revealing that mannose/glucose residues are homogeneously distributed on the surface. (**c**) AFM topographic image recorded in PBS showing two *M. bovis* BCG cells on a polymer substrate. (**d**) Representative adhesion force map (*gray scale*: 100 pN) recorded with a heparin-modified AFM tip. Adhesion events (*bright pixels*) reflect the detection of single cell adhesion proteins (HBHA), which apparently are concentrated into nanodomains. (**e**) AFM image of *Lactococcus lactis* cells during the course of the division process, showing a well-defined division septum rich in nascent peptidoglycan. (**f**) Adhesion force map (gray scale: 100 pN) recorded with a vancomycin tip on the septum region. Adhesion events were essentially located in the septum region (*dashed line*), suggesting newly formed peptidoglycan is inserted there. Reprinted with permission from [28] and from [29]
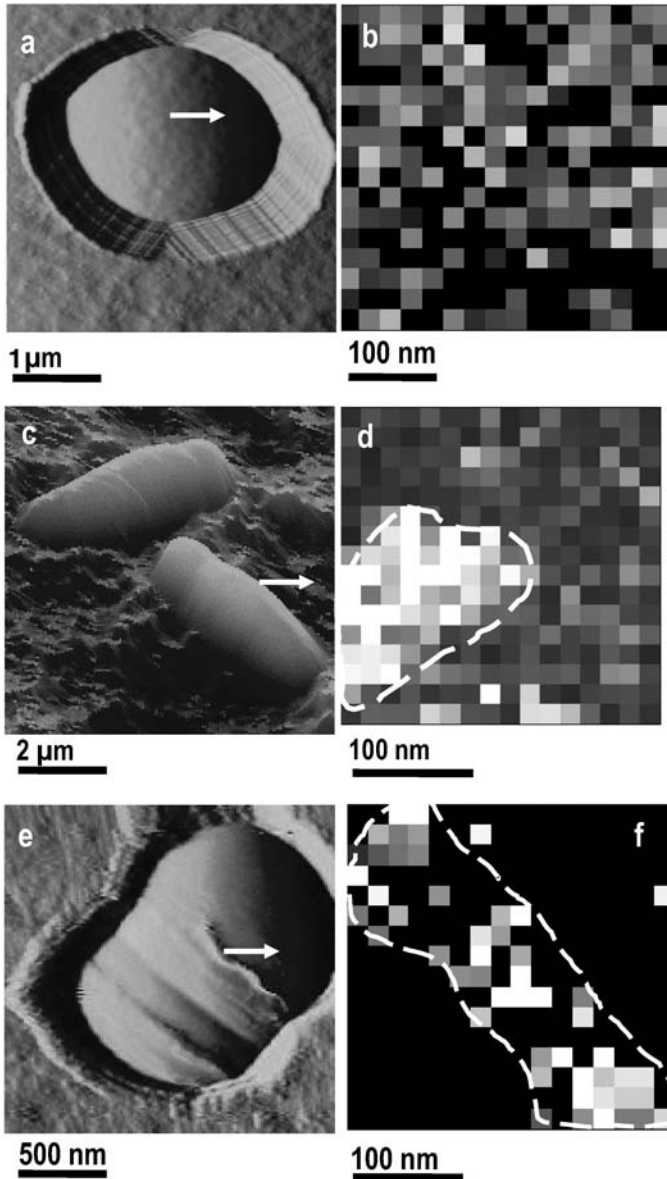
Fig. 10.6.

of the locations. The adhesion force magnitude was very close to the value of single HBHA–heparin interactions, supporting the notion that single adhesins were detected. This was further confirmed by showing that a mutant strain lacking HBHA did not bind the heparin tip. Interestingly, the HBHA distribution was not homogeneous, but apparently concentrated into nanodomains which may promote adhesion to target cells by inducing the recruitment of receptors within membrane rafts. In

the future, these molecular recognition studies may help in the development of new drugs capable to block bacterial adhesion.

More recently, spatially resolved SMFS with antibiotic-modified tips was used to map individual binding sites on live bacteria (Fig. 10.6e, f; [29]). Fluorescence microscopy with a fluorescent vancomycin probe was used to visualize D-Ala-D-Ala sites of nascent peptidoglycan in the cell wall of dividing *Lactococcus lactis* cells. Fluorescence staining of the wild-type strain was found around the septum, while no fluorescent labeling was detected for a mutant strain producing peptidoglycan precursors ending by D-Ala-D-Lac instead of D-Ala-D-Ala. AFM topographic images of *L. lactis* cells revealed a smooth and elongated cell morphology as well as a well-defined division septum (Fig. 10.6e). Ring-like structures were seen at a certain distance from the septum, presumably formed by an outgrowth of the cell wall. Notably, adhesion force maps demonstrated that binding sites were essentially located in the septum region, and more specifically on the equatorial rings (Fig. 10.6f), suggesting that newly formed peptidoglycan was inserted in these regions. This study shows that AFM with vancomycin tips is a complementary approach to fluorescent vancomycin to explore the architecture and assembly process of peptidoglycan during the cell cycle of Gram-positive bacteria. While fluorescence microscopy generates microscale images allowing the localization of peptidoglycan in the entire cell wall, AFM adhesion force mapping reveals the distribution of single peptidoglycan molecules on the outermost cell surface.

While spatially resolved SMFS provides a quantitative analysis of unbinding forces, it is limited by its time resolution. The time currently required to record a map is on the order of 2–15 min depending on the acquisition parameters, which is much greater than the time scale at which dynamic processes usually occur in biology. An exciting alternative in this context is dynamic recognition force mapping (TREC) [30] which records topography and recognition images at the same speed as that used for conventional topographic imaging, typically 1–2 images per minute. Recently, Chtcheglova et al. [31] applied TREC imaging to microvascular endothelial cells to demonstrate that cadherins, involved in homophilic cell-to-cell adhesion, are organized into nanodomains ranging from 10 to 100 nm in diameter. Clearly, a challenging issue for future research would be to apply TREC imaging in the microbiological context.

10.3.2
Immunogold Imaging

A different way of exploiting molecular recognition for AFM imaging is to use immunogold labels as cell-surface markers, as is traditionally used in electron microscopy. Here, cells are first incubated with monoclonal antibodies directed against specific cell wall constituents, then further incubated with the corresponding gold-conjugated secondary antibodies, and finally imaged using topographic imaging. In pioneering work [32], application of the approach to dried immunogold-labeled human lymphocytes enabled researchers to resolve the location of antigens on the cell surface. Similarly, types I and II collagen fibers were revealed on dried rat fibroblasts and human chondrosarcoma cells [33]. For the first time, immunogold
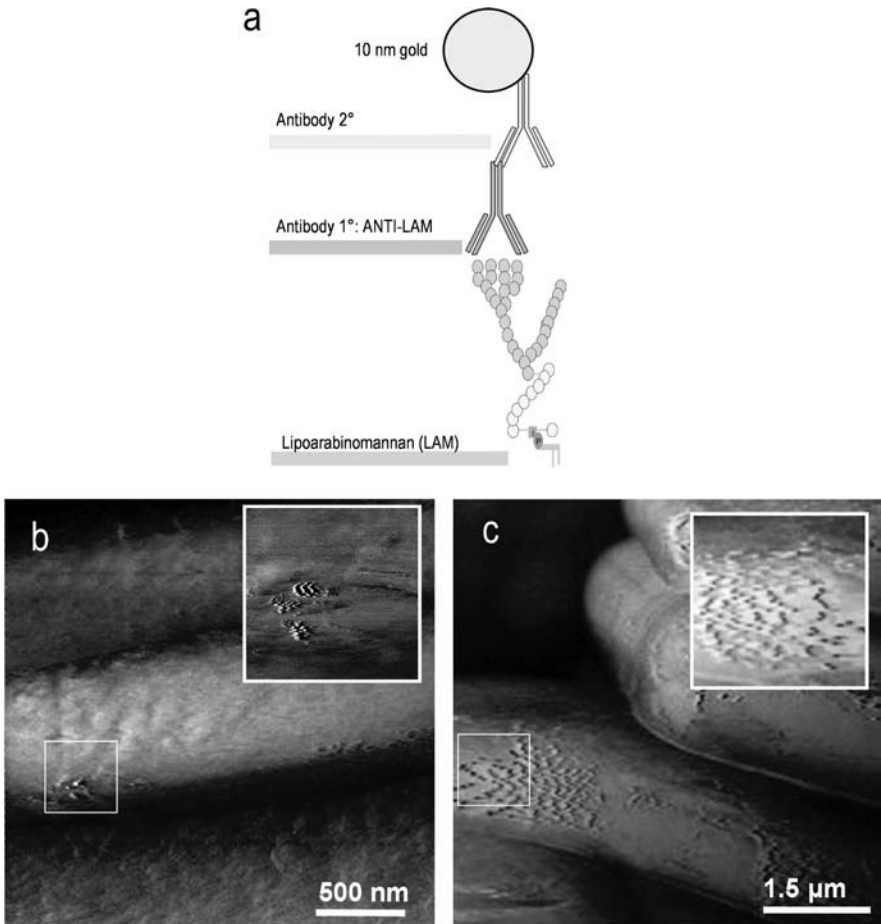
Fig. 10.7. Molecular recognition imaging of live cells using immunogold labeling. (**a**) *M. bovis* BCG cells were incubated with monoclonal anti-LAM antibodies, followed by another incubation with the corresponding gold-conjugated secondary antibodies. (**b**, **c**) AFM tapping mode (phase) images of immunogold-labeled cells prior (**b**) and after (**c**) treatment for 24 h with isoniazid, revealing that the drug induces the massive exposure of LAM at the surface. Reprinted with permission from [18]

AFM imaging was used to detect and localize lipoarabinomannan (LAM) on the surface of live, hydrated mycobacteria (Fig. 10.7) [18]. Contact mode and tapping mode images were obtained prior and after treatment with two antibiotics, INH and EMB. Gold particles were never seen in contact mode, emphasizing the need to use tapping (phase) mode for such in situ immunogold studies. Using tapping mode, the surface of native cells showed essentially no labeling, suggesting that LAM is not exposed at the surface. This finding was consistent with the uniform distribution of cell surface hydrophobicity measured on native cells. By contrast, INH and EMB-treated cells revealed a large coverage of gold particles, indicating that LAM was exposed. This

observation, which correlates with topographic and CFM data, provides direct evidence that the two drugs lead to the massive exposure of LAM at the cell surface. In summary, this study showed that combining immunogold detection with topographic imaging and CFM allows us to shed new light into the 3-D organization of bacterial cell walls.

10.4
Conclusions

Owing to its ability to observe and manipulate biosystems under physiological conditions, AFM is revolutionizing the way in which today researchers explore live cells. Here, we have shown that two AFM modalities, CFM and molecular recognition imaging, offer fascinating prospects for mapping the chemical and biochemical properties of live cells. These nanoscale analyses should have an important impact on future life science and biomedical research, particularly to understand the molecular bases of cell–drug and host–pathogen interactions. Yet, it must be realized that procedures for attaching chemical groups, biomolecules and cells to AFM cantilevers remain labor intensive and require specific expertise that is usually not found in biology laboratories. In the future, defining simple standard protocols for tip functionalization and making them readily available to the biological community should contribute to spread the use of force spectroscopy in the various life science disciplines.

References

1. Fritz J, Baller MK, Lang HP, Rothuizen H, Vettiger P, Meyer E, Guntherodt HJ, Gerber C, Gimzewski JK (2000) Science 288:316
2. Turner APF (2000) Science 290:1315
3. Niemeyer CM, Mirkin CA (2004) Nanobiotechnology: Concepts, applications and persepectives. VCH (ed). Wiley, Weinheim, p 469.
4. Jahn TR, Radford SE (2005) FEBS J 272:5962
5. Doyle RJ (2000) Microb Infect 2:391
6. Noy A (2006) Surf. Interface Anal 38:1429
7. Smith SB, Finzi L, Bustamante C (1992) Science 258:1122
8. Ashkin A, Schutze K, Dziedzic JM, Euteneuer U, Schliwa M (1990) Nature 348:346
9. Vezenov DV, Noy A, Ashby P (2005) J Adhes Sci Technol 19:313

10. Burnham NA, Chen X, Hodges CS, Matei GA, Thoreson EJ, Roberts CJ, Davies MC, Tendler SJB (2003) Nanotechnology 14:1
11. Noy A, Frisbie CD, Rozsnyai LF, Wrighton MS, Lieber CM (1995) J Am Chem Soc 117:7943
12. vanderVegte EW, Hadziioannou G (1997) Langmuir 13:4357
13. Vezenov DV, Noy A, Rozsnyai LF, Lieber CM (1997) J Am Chem Soc 119:2006
14. Frisbie CD, Rozsnyai LF, Noy A, Wrighton MS, Lieber CM (1994) Science 265:2071
15. Sinniah SK, Steel AB, Miller CJ, ReuttRobey JE (1996) J Am Chem Soc 118:8925
16. Cappella B, Dietler G (1999) Surf Sci Rep 34:1
17. Alsteens D, Dague E, Rouxhet PG, Baulard AR, Dufrêne YF (2007) Langmuir 23:11977
18. Alsteens D, Verbelen C, Dague E, Raze D, Baulard AR, Dufrêne YF (2008) Eur J Physiol 456:117
19. Dague E, Alsteens D, Latge JP, Verbelen C, Raze D, Baulard AR, Dufrêne YF (2007) Nano Lett 7:3026
20. Dupont-Gillain CC, Nysten B, Hlady V, Rouxhet PG (1999) J Colloid Interface Sci 220:163
21. Ducker WA, Senden TJ, Pashley RM (1991) Nature 353:239
22. Ahimou F, Denis FA, Touhami A, Dufrene YF (2002) Langmuir 18:9937
23. Dague E, Alsteens D, Latgé JP, Dufrêne YF (2008) Biophys J 94:656
24. Ludwig M, Dettmann W, Gaub HE (1997) Biophys J 72:445
25. Grandbois M, Dettmann W, Benoit M, Gaub HE (2000) J Histochem Cytochem 48:719
26. Lehenkari PP, Charras GT, Nykänen A, Horton MA (2000) Ultramicroscopy 82:289
27. Almqvist N, Bhatia R, Primbs G, Desai N, Banerjee S, Lal R (2004) Biophys J 86:1753
28. Dupres V, Menozzi FD, Locht C, Clare BH, Abbott NL, Cuenot S, Bompard C, Raze D, Dufrêne YF (2005) Nat Methods 2:515
29. Gilbert Y, Deghorain M, Wang L, Xu B, Pollheimer PD, Gruber HJ, Errington J, Hallet B, Haulot X, Verbelen C, Hols P, Dufrene YF (2007) Nano Lett 7:796
30. Raab A, Han WH, Badt D, Smith-Gill SJ, Lindsay SM, Schindler H, Hinterdorfer P (1999) Nat Biotechnol 17:902
31. Chtcheglova LA, Waschke J, Wildling L, Drenckhahn D, Hinterdorfer P (2007) Biophys J 93:L11
32. Putman CAJ, Degrooth BG, Hansma PK, Vanhulst NF, Greve J (1993) Ultramicroscopy 48:177
33. Arntz Y, Jourdainne L, Greiner-Wacker G, Rinckenbach S, Ogier J, Voegel JC, Lavalle P, Vautier D (2006) Microsc Res Tech 69:283